Supporting Information

Mauvoisin et al. 10.1073/pnas.1314066111

SI Materials and Methods

Animals. All animal studies were conducted in accordance with the regulations of the veterinary office of the Canton of Vaud. C57BL/6J mice were purchased from Charles River Laboratory. *Cry1*/*Cry2* double KO mice (1) in the C57BL/6J genetic background have been previously described (2). In all experiments, male mice between 10 and 12 wk of age were used. Unless noted otherwise, mice were maintained under standard animal housing conditions with free access to food and water in 12-h light–dark (LD) cycles. However, for all experiments, animals were fed only at night starting 4 d before the experiment to control for genotype-dependent feeding rhythms.

Experiments in constant darkness (DD) with or without starvation (DD starved) were conducted like in our previous study (3). Briefly, during the last dark period, mice were deprived from food (starvation) or had access to food ad libitum. Thereafter, mice were shifted into complete darkness and then, killed every 4 h during the next 24 h.

For the establishment of stable isotope labeling by amino acids (SILAC) mice, C57BL/6J mice were fed for two generations with L-lysine $^{13}C_6$ chow diet (Cambridge Isotope Laboratories, Inc.) as described previously (4). Measurements by MS of blood albumin and tail collagen labeling of the mice confirmed a more than 97% incorporation of the heavy isotope (Fig. S2).

Protein Extracts. Livers were homogenized in lysis buffer containing 8 M urea, a protease inhibitor mixture (cOmplete ULTRA; 05892970001; Roche), and a phosphatase inhibitor mixture (PhosphoSTOP; 04906837001; Roche). After 20 min of incubation on ice, extracts were centrifuged for 10 min at 20,000 × *g*. The supernatants were harvested, and the resulting total protein extracts were quantified using a BCA protein assay kit (Thermo).

Western Blotting. Thirty micrograms total protein extracted from liver of WT mice were used for Western blotting according to standard procedures. Densitometry analyses of the blots were performed using the ImageJ software. For the Western blots performed on liver samples, naphtol blue-black staining of the membranes was used as a loading control and serves as a reference for normalization of the quantified values. For the Western blots on plasma samples, because total protein concentration changes according to the time of day (5), it was not possible to normalize to an internal loading control. We, thus, normalized the loading to the volume of plasma loaded on each well. References for the antibodies are given in Table S1.

SILAC MS. Equal amounts of proteins extracted from two non-SILAC mice were pooled for 16 time points (every 3 h for 45 h; WT mix). A complex and common reference SILAC protein mix (SILAC mix) was prepared from 16 SILAC protein samples (6 SILAC male and 10 SILAC female livers) collected at Zeitgeber time 0 (ZT0) and ZT12 (Fig. S1). Thereafter, 16 mixes were obtained by adding the same amount of SILAC mix to the WT mixes. An equivalent procedure was applied for four *Cry1*/*Cry2* KO mice protein samples collected every 6 h for 24 h, and the same SILAC mix was used as a reference. Mixed samples were reduced with DTT and alkylated with iodoacetamide. After an ethanol–acetate precipitation, they were resuspended in 250 mM triethylammonium bicarbonate (pH 8.0) containing 4 M urea and digested overnight at 37 °C with trypsin. The obtained peptide mixtures (250 μg total material) were desalted on SepPak C18 cartridges (Waters Corp.), dried, dissolved in 4 M urea with 0.1% ampholytes (pH 3–10; GE Healthcare), and fractionated by off-gel focusing as described (6). Twenty fractions obtained were desalted on a microC18 96-well plate (Waters Corp.), dried, and resuspended in 0.1% formic acid and 3% (vol/vol) acetonitrile for liquid chromatography (LC)-MS/MS analysis. Samples were analyzed on a hybrid linear trap LTQ-Orbitrap Velos mass spectrometer (Thermo Fisher) interfaced through a nanospray source to a Dionex RSLC 3000 nanoHPLC system (Dionex). Peptides were separated on a reversed phase Acclaim Pepmap nanocolumn (75 μm internal diameter × 25 cm, 2.0 μm, 100 Åμ; Dionex) with a gradient from 5% to 85% (vol/vol) acetonitrile in 0.1% formic acid (total time = 120 min) and a flow rate of 0.3 μL/min. Full MS survey scans were performed at 60,000 resolution. In data-dependent acquisition controlled by Xcalibur 2.1 software (Thermo Fisher), the 20 most intense multiply-charged precursor ions detected in the full MS survey scan were selected for collision-induced dissociation (CID) fragmentation in the LTQ linear trap with an isolation window of 3.0 *m*/*z* and then, dynamically excluded from additional selection during 120 s.

MS Data Analysis. MS data were analyzed and quantified with MaxQuant version 1.3.0.5 (7) using Andromeda as search software (8) against the UniProt (release 2012_02) database restricted to Mouse (*Mus musculus*) taxonomy and a custom database containing the usual contaminants (digestion enzymes, keratins, etc.). Cleavage specificity was trypsin/P (cleavage after Lysine and Arginine, including Lysine-Proline and Arginine-Proline) with two missed cleavages. Mass tolerances were 6 ppm for the precursor and 0.5 Da for CID MS/MS. The iodoacetamide derivative of cysteine was specified as a fixed modification, and oxidation of methionine and protein N-terminal acetylation were specified as variable modifications. Protein identifications were filtered at 1% false discovery rate (FDR) established by MaxQuant against a reversed sequence database. A minimum of one unique peptide was necessary to discriminate sequences that shared peptides. Sets of protein sequences that could not be discriminated based on identified peptides were listed together as protein groups and are fully reported in Dataset S1. Details of peak quantitation and protein ratio computation by MaxQuant are described elsewhere (7).

Detection of Rhythmic Proteins. After removal of contaminant proteins and hits against decoy sequences, we assessed rhythmicity in protein expression profiles using harmonic regression. Specifically, we focused on 24-h periodicity only (data are generated under 24-h LD cycles) by performing a multiple linear regression for each relative protein time trace (transformed to log2 units). For this analysis, we used the relation $y(t) = \mu + a\cos(2\pi/24 \times t) + b\sin(2\pi/24 \times t)$ + noise, with $y(t)$ as the dependent variable and $x_1 = \cos(2\pi/24 \times t)$ and $x_2 = \sin(2\pi/24 \times t)$ as the explanatory variables; μ is the mean, whereas a and b are the coefficients of cosine and sine functions with period of 24 h, respectively. These coefficients determine the peak–trough amplitude $2\sqrt{a^2+b^2}$, the relative amplitude (maximum minus minimum divided by two times the mean), $\sqrt{a^2+b^2}/\mu$, and the tangent of the phase b/a. To test for statistical significance against the null hypothesis that $a = 0$ and $b = 0$, we use the standard F test for linear regression. Analysis with the Jonckheere-Terpstra-Kendall cycle provided very similar results. Note also that biological replicas can be readily taken into account: each replica counts for one entry in the vectors x_1, x_2, and y. Finally, the resulting P values of all proteins are used to

estimate FDR by the Benjamini–Hochberg method (9). All test statistics are provided in Dataset S1.

Microarray Analysis. To analyze the relationship between mRNA and protein accumulation profile, we used our previously published microarray data of mRNAs in mouse liver containing 48 arrays of 2-h resolution for two biological replicas under ZT conditions and identical feeding regimen, which is available in the Gene Expression Omnibus database (accession no. GSE33726) (3). The raw data are normalized together by the robust multiarray average method (10). To determine the subset of rhythmic mRNAs, we used the same above tests and FDR calculations. We then used the Affymetrix annotation (Mouse430_2.na33.annot.csv) to establish the mapping between mRNA probe sets and measured proteome by the gene name. Some proteins may have several matched mRNA probe sets. In this case, we selected the most rhythmic probe set (with the lowest q value) (Fig. S4).

Protein Half-Lives. To compare the protein half-lives in different classes, we used data from NIH 3T3 cells (11). The mapping was done by the gene names and Uniprot identifications. We used the average protein half-life from the published data (included in Dataset S1).

Statistical Tests. For the comparison of protein accumulation profiles in WT and *Cry1*/*Cry2* KO mice, we used the Pearson coefficient (R) to measure the correlation (Fig. 4*A*). Because the *Cry1*/*Cry2* KO mice data were obtained at four time points (ZT0, ZT6, ZT12, and ZT18), we used the average of WT duplicates of the same time points to calculate the correlation. P values are given by $P = 1 - (R + 1)/2$ (Dataset S1). To assess differences between class 3 (C3) and C4, we used the Kolgomorov–Smirnov test (Fig. 4*B*).

Model for Protein Accumulation. To quantify the amplitude and phase relationships in proteins and mRNA profiles, we model protein accumulation profiles $p(t)$ assuming a constant protein half-life:

$$\frac{dp}{dt} = \beta m(t) - \gamma p$$

$$m(t) = m_0(1 + b\cos\omega t)$$

$$\Rightarrow$$

$$p(t) = \frac{\beta m_0}{\gamma}(1 + B\cos(\omega t - \phi))$$

$$\tan(\phi) = \frac{\omega}{\gamma} = \frac{\pi}{12[h]}\frac{\tau_{half}}{\ln 2}$$

$$\frac{B}{b} = \cos(\phi) = \frac{1}{\sqrt{\left(\frac{\omega}{\gamma}\right)^2 + 1}}.$$

Here, $m(t)$ is the accumulation profile of mRNA described by a cosine function with a frequency of $\omega = 2\pi/24[h]$, and characterized by three parameters: the mean m_0, the relative amplitude b, and the phase, which is taken as zero here for simplicity; β, γ, and τ_{half} represent the translation rate, the degradation rate of protein assumed to be constant, and the protein half-life, respectively. This model predicts that the protein accumulation also follows a cosine function with mean $\beta m_0/\gamma$, relative amplitude B, and delay ϕ. The translation rate affects only the mean of the protein accumulation. The tangent of the delay is given by the ratio of frequency to the degradation rate. Therefore, for a very short half-life protein, the delay approaches 0 h, and for a long half-life protein, the delay becomes maximally 6 h. Moreover, the ratio of relative amplitudes B/b is the cosine of the phase delay, meaning that the ratio is one for short-lived proteins and zero for long-lived proteins.

Gene Ontology. The analysis of protein function is performed using the DAVID Bioinformatics Resources 6.7 at http://david.abcc.ncifcrf.gov/. In Dataset S2, we provide the functional annotation clusters for C3 and C4 genes that showed enrichment above 1.5 compared with the entire mouse proteome.

1. van der Horst GTJ, et al. (1999) Mammalian Cry1 and Cry2 are essential for maintenance of circadian rhythms. *Nature* 398(6728):627–630.
2. Bur IM, et al. (2009) The circadian clock components CRY1 and CRY2 are necessary to sustain sex dimorphism in mouse liver metabolism. *J Biol Chem* 284(14):9066–9073.
3. Jouffe C, et al. (2013) The circadian clock coordinates ribosome biogenesis. *PLoS Biol* 11(1):e1001455.
4. Krüger M, et al. (2008) SILAC mouse for quantitative proteomics uncovers kindlin-3 as an essential factor for red blood cell function. *Cell* 134(2):353–364.
5. Scheving LE, Pauly JE, Tsai TH (1968) Circadian fluctuation in plasma proteins of the rat. *Am J Physiol* 215(5):1096–1101.
6. Geiser L, Dayon L, Vaezzadeh AR, Hochstrasser DF (2011) Shotgun proteomics: A relative quantitative approach using Off-Gel electrophoresis and LC-MS/MS. *Methods Mol Biol* 681:459–472.
7. Cox J, Mann M (2008) MaxQuant enables high peptide identification rates, individualized p.p.b.-range mass accuracies and proteome-wide protein quantification. *Nat Biotechnol* 26(12):1367–1372.
8. Cox J, et al. (2011) Andromeda: A peptide search engine integrated into the MaxQuant environment. *J Proteome Res* 10(4):1794–1805.
9. Benjamini Y, Hochberg Y (1995) Controlling the false discovery rate: A practical and powerful approach to multiple testing. *J R Statist Soc B* 57(1):289–300.
10. Irizarry RA, et al. (2003) Exploration, normalization, and summaries of high density oligonucleotide array probe level data. *Biostatistics* 4(2):249–264.
11. Schwanhäusser B, et al. (2011) Global quantification of mammalian gene expression control. *Nature* 473(7347):337–342.

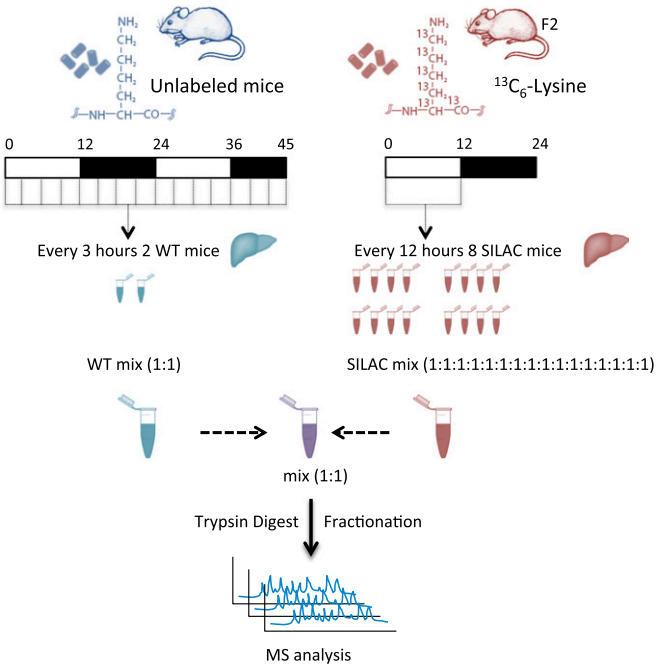

Fig. S1. Experimental design of the SILAC proteomics experiment. Workflow followed for SILAC MS analysis of mouse liver protein extracts.

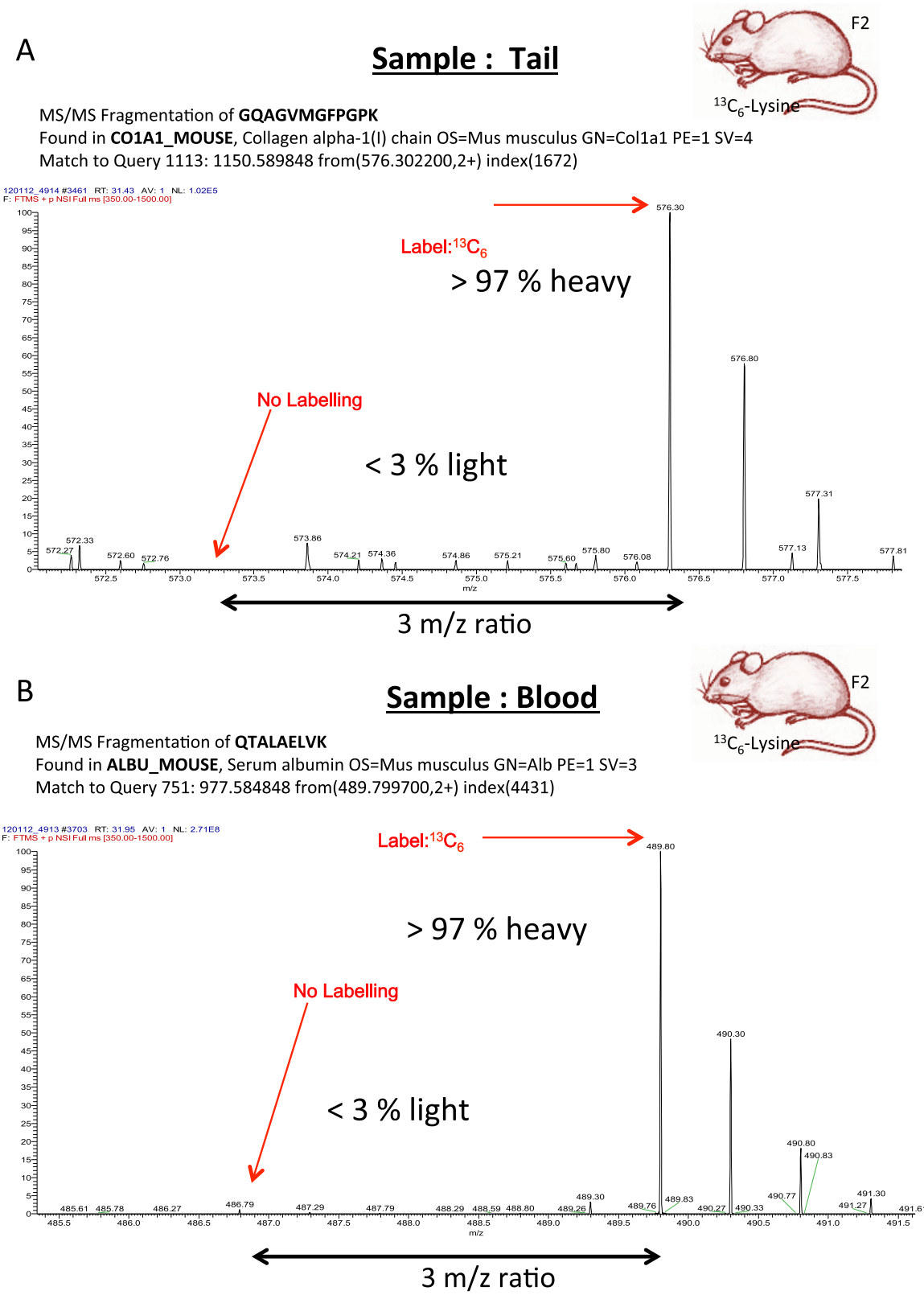

Fig. S2. Extent of isotope labeling of mouse tissues. (*A*) Tail and (*B*) serum samples were collected from SILAC animals. Tail proteins were extracted by mechanical homogenization in 8 M urea buffer (like for the liver samples) and separated by 1D electrophoresis. Random gel regions (tail; collagen-1-α) and the albumin band (plasma) were in-gel digested with Trypsin and analyzed by MS. Labeling of Lys-containing peptides was found to be >97% for all proteins identified in both samples.

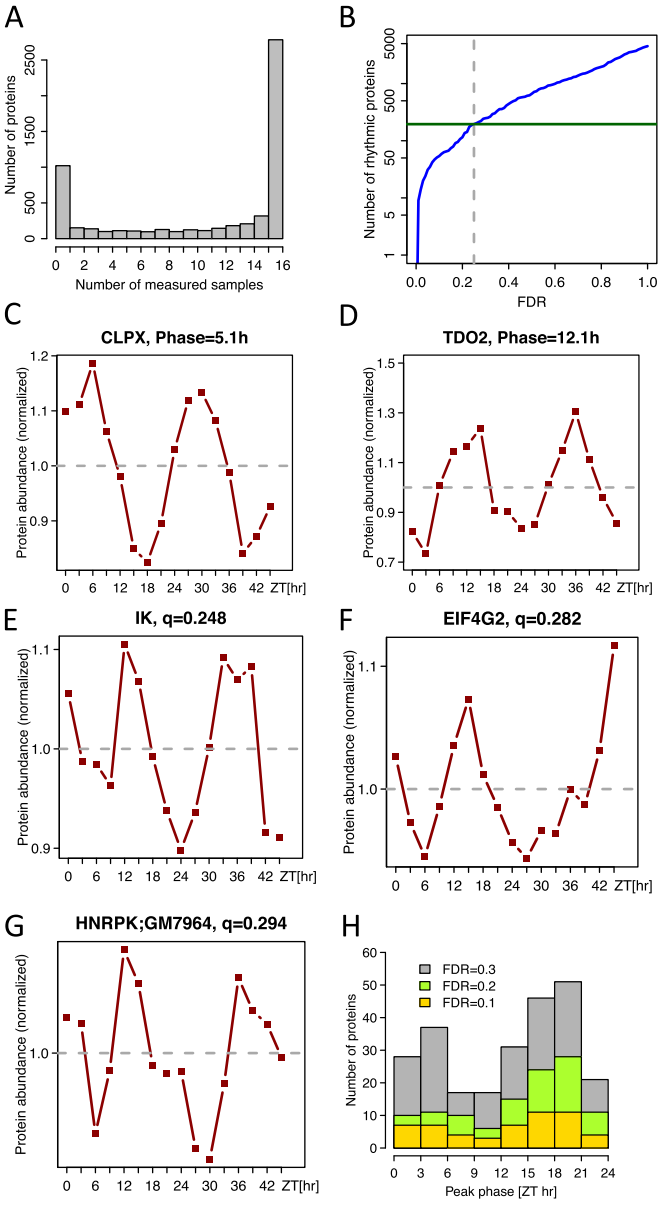

Fig. S3. Identification of rhythmic proteins with the temporal profiles of relative abundances in mouse liver. (*A*) Distribution of sample numbers quantified for the total 5,827 proteins. (*B*) Dependency of the number of rhythmic proteins in the function of FDR. With a value of FDR < 0.25, 195 rhythmic proteomes are identified (green line). (*C* and *D*) Examples of rhythmic proteins encoded by individual genes (data are normalized to the temporal mean). (*E*–*G*) Examples of proteins with *q* values between 0.24 and 0.3. (*H*) Phase distribution for the rhythmic proteins is similar for different FDRs (0.3, 0.2, and 0.1).

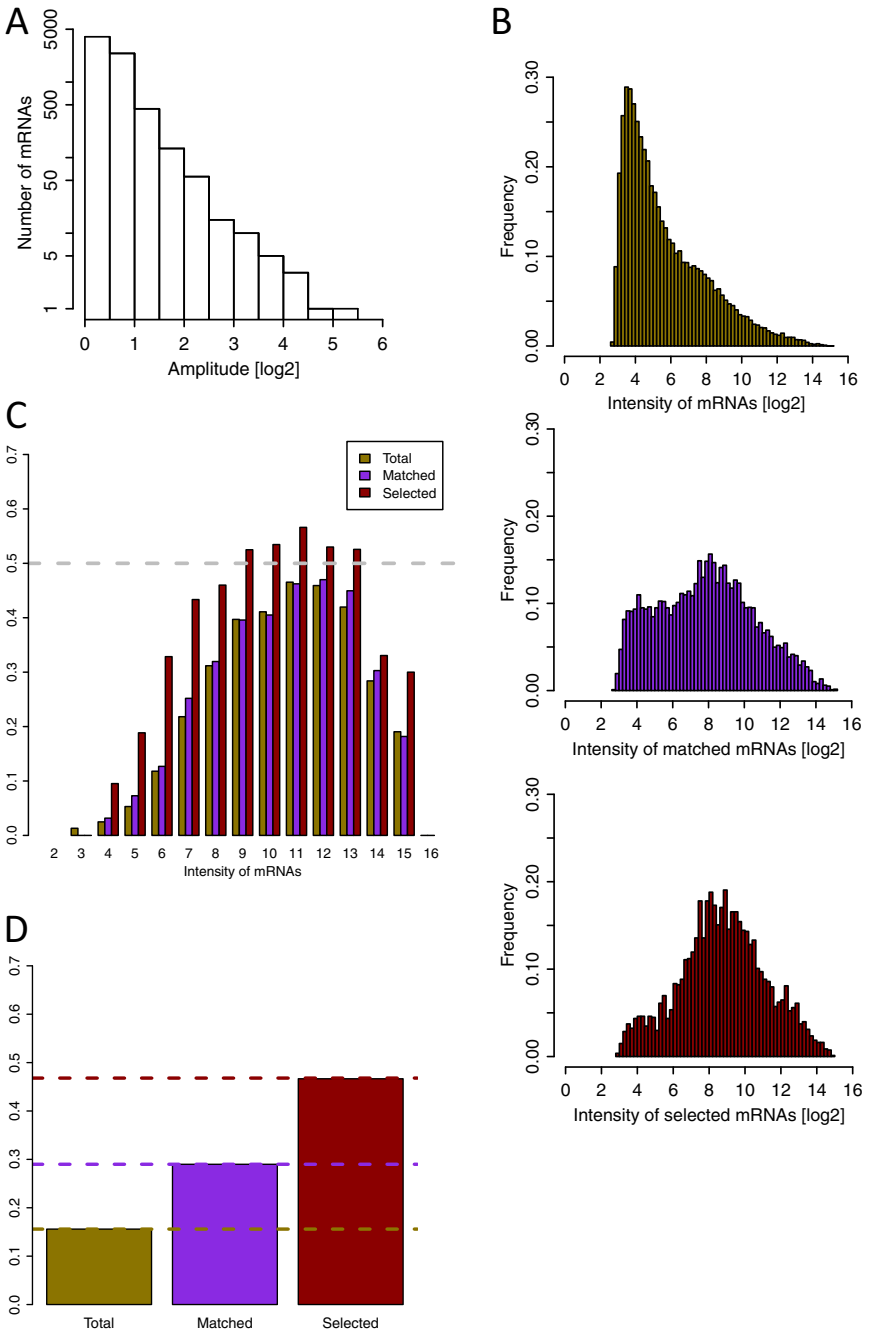

Fig. S4. Explanation for the percentage of rhythmic mRNAs corresponding to measured proteins. (*A*) Distribution of peak-to-trough amplitude (log2 units) for all rhythmic mRNAs with FDR < 0.05. Comparison with the protein amplitudes (Fig. 1*C*) shows that mRNA amplitudes are, on average, significantly higher than proteins amplitudes. (*B*) Temporal average of mRNA intensity for all mRNA probe sets (gold), probe sets that matched measured protein according to annotation (violet; several probe sets may match a given protein), and one selected probe set for each protein showing the best diurnal cycling or lowest *q* value among all matched probe sets (red). Expectedly, the matched probe sets are enriched in high mRNA intensities, and the selected probe sets are also further shifted to higher intensity. (*C*) Percentage of rhythmic mRNAs (FDR < 0.05) in function of mRNA signal intensity for all, matched, and selected mRNAs. The percentages reach ∼45% and ∼11% at intensities for all and matched probe sets, respectively; moreover, selecting the most rhythmic probe for each protein further increases the percentage by ∼10% for each intensity bin. (*D*) Combining *B* and *C* explains why the percentage of rhythmic mRNAs after the selection (red) is ∼45%. The estimate of 15% genome-wide (gold) is consistent with previous publications.

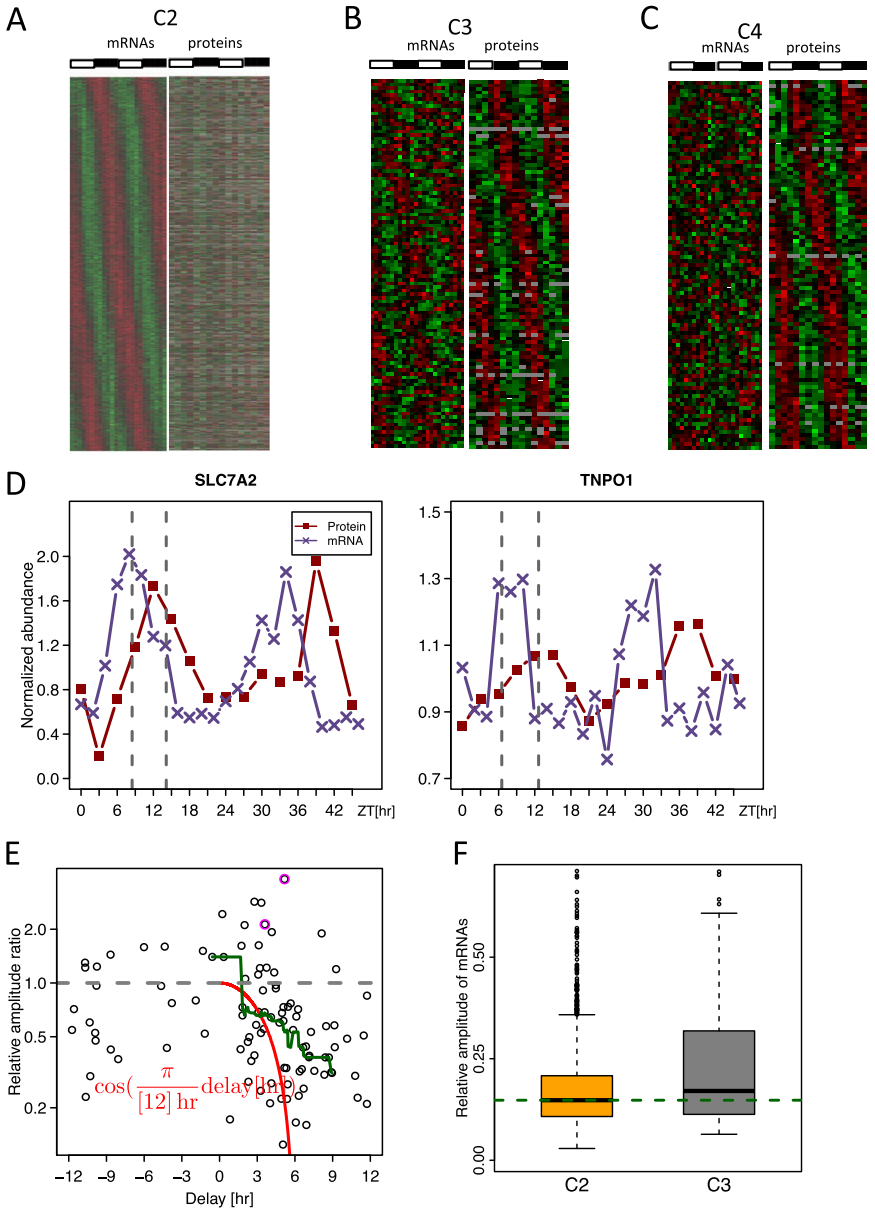

Fig. S5. Relationship between mRNA and protein accumulation profiles. (*A*–*C*) Heatmap representations of proteins and mRNAs in C2–C4. Data are standardized by rows, and gray blocks indicate missing data. (*D*) Individual examples of delayed protein vs. mRNA profiles. Gray lines indicate estimated peak times from cosine fits. (*E*) Relationship between the ratio of relative amplitudes in protein to mRNA and the phase delay. The red line shows expected result when the protein half-life is assumed constant. In that case, the delay must be in the interval from 0 (very short-lived proteins) to 6 h (longest-lived proteins). The green line shows the moving median in the window −1 to 9 h. Two examples of outliers (indicated by magenta circles) are shown in Fig. S6*B*. (*F*) Relative amplitude of mRNA oscillations in C2 and C3.

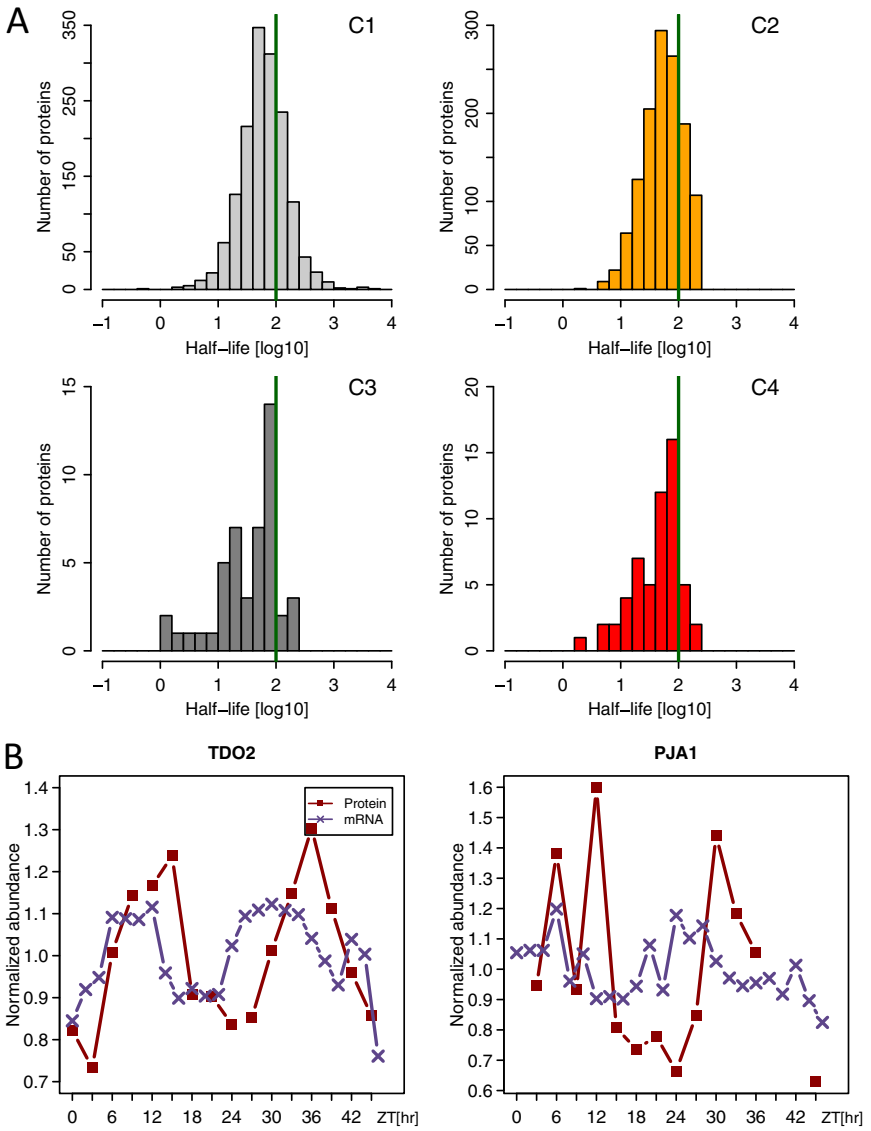

Fig. S6. Distribution of protein half-lives and representative examples of rhythmic proteins showing posttranslational regulation. (*A*) Distributions of protein half-lives (measured in NIH 3T3 cells) (1) in four classes indicate that short-lived proteins are enriched in C3 and C4 (rhythmic proteins) compared with C1 and C2 (nonrhythmic proteins). (*B*) Individual examples (Fig. S5*E*, magenta circles) in which protein rhythms show higher amplitudes than their corresponding mRNAs.

1. Schwanhäusser B, et al. (2011) Global quantification of mammalian gene expression control. *Nature* 473(7347):337–342.

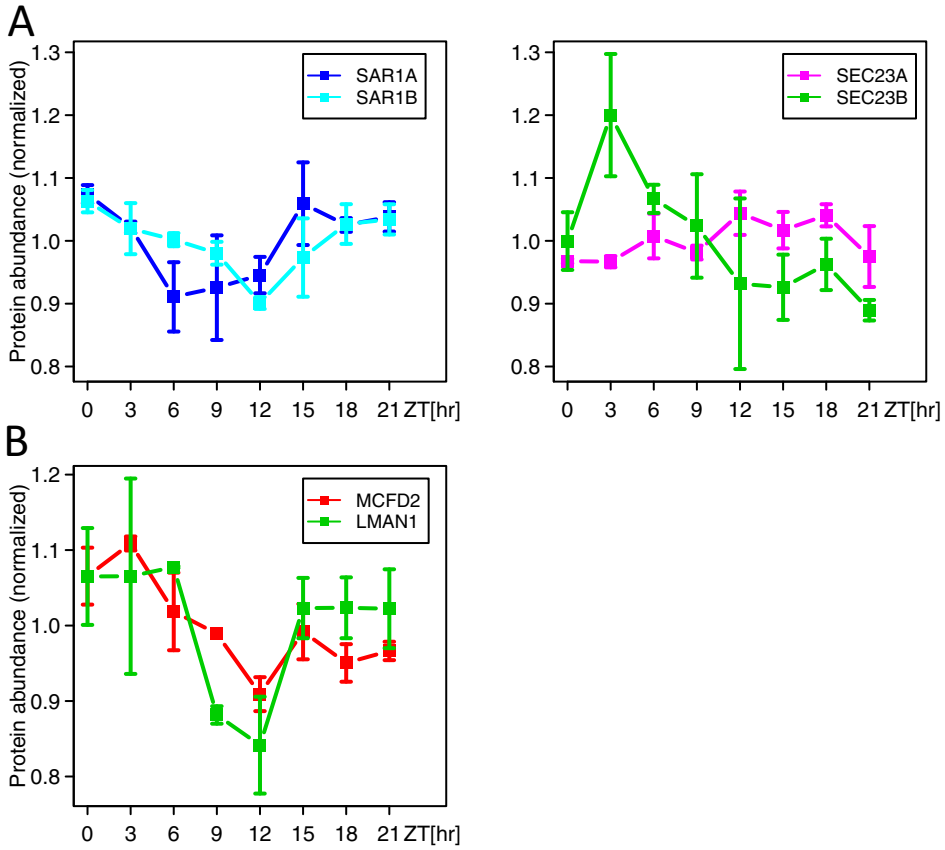

Fig. S7. Diurnal protein measurements for the proteins involved in the (*A*) COPII complex and (*B*) the endoplasmic reticulum cargo receptor complex. MS statistics for the genes are $P = 0.17$ and $q = 0.26$ for SAR1A, $P = 0.0059$ and $q = 0.19$ for SAR1B, $P = 0.072$ and $q = 0.43$ for SEC23A, $P = 0.034$ and $q = 0.34$ for SEC23B, $P = 0.047$ and $q = 0.39$ for MCFD2, and $P = 0.050$ and $q = 0.40$ for LMAN1.

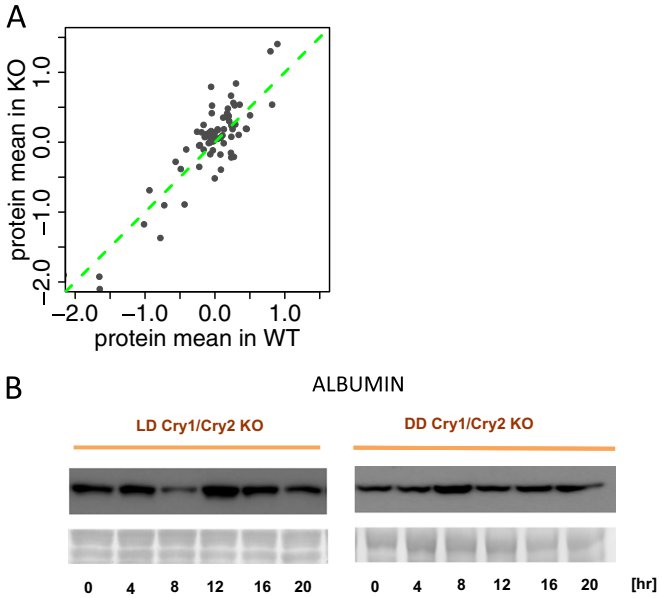

Fig. S8. Protein expression in *Cry1/Cry2* KO mice. (*A*) Comparison of mean protein levels in WT and *Cry* KO (our MS data) for C3 proteins shows no systematic differences. (*B*) Temporal levels of ALBUMIN in the liver of *Cry1/Cry2* KO mice. Western blots performed with liver extracts from *Cry1/Cry2* KO mice in (*Left*) LD condition or (*Right*) DD.

Table S1. Reference of antibodies used for Western blotting

Protein	Ref.	Company
ALB	16475–1-AP	ProteinTech
PCK1	16754–1-AP	ProteinTech
PLIN2	LS-C141373	Lifespan Bioscience
SERPINA1 (used for plasma WB)	CPBT-27482MM	Creative Diagnostics
SERPINA1 (used for liver WB)	HPA000927	Sigma
TFR2	sc-48747	Santa-Cruz

Dataset S1. Proteomics data

Dataset S1

(Sheet 1) Relative abundance (ratio H/L normalized from the MaxQuant analysis) for all distinct 5,827 proteins identified by SILAC MS in mouse liver under ZT conditions. Time resolution is 3 h (eight time points per day and two biological replicas; replica one spans from ZT00 to ZT21, and replica two spans from ZT24 to ZT45). Of 5,827 proteins, 70% yielded a sufficient number of peptides, permitting the estimation of relative abundances in at least 8 of 16 time points. The rhythmicity analysis for those proteins is provided. (Sheet 2) Data for the set of 4,408 measured proteins with the corresponding mRNA probe set (in case of multiple matches, we selected the probe set with lowest rhythmicity q value for each protein) and expression data covering 2 ZT d at 2-h time resolution. The rhythmicity analysis for proteins and mRNA is also provided. (Sheet 3) SILAC MS data measured in *Cry1*/*Cry2* KO arrhythmic mice under night-restricted feeding. Data comprise four time points spanning 1 ZT d at 6-h time resolution. Correlation analysis between *Cry1*/*Cry2* KO and WT mice is provided.

Dataset S2. Gene ontology analysis

Dataset S2

(Sheet 1) Functional clustering analysis for rhythmic proteins with accumulation phases between 0 and 12 h in C3 (genes with rhythmic mRNAs and rhythmic proteins). (Sheet 2) Functional clustering analysis for rhythmic proteins with accumulation phases between 12 and 24 h in C3 (genes with rhythmic mRNAs and rhythmic proteins). (Sheet 3) Functional clustering analysis for rhythmic proteins with accumulation phases between 0 and 12 h in C4 (with rhythmic proteins but flat mRNAs). (Sheet 4) Functional clustering analysis for rhythmic proteins with accumulation phases between 12 and 24 h in C4 (with rhythmic proteins but flat mRNAs) shows enrichment of secreted proteins.

Dataset S3. List of secreted proteins (53 in total) detected in mouse liver, of which 39 proteins passed our threshold for rhythmic accumulations (FDR < 0.25)

Dataset S3